Phase relations in the system anorthite–potassium-feldspar at 10 kbar with emphasis on their solid solutions

Y. AI AND D. H. GREEN

Department of Geology, University of Tasmania, Australia

Abstract

Phase relations in the binary system anorthite–K-feldspar at 10 kbar were studied with a solid-media piston cylinder apparatus. The eutectic character of this system is confirmed, with the eutectic point located at $An_{30}Kf_{70}$ (± 3 mol%), and 1215 ± 15 °C, 10 kbar. The mutual solubilities between anorthite and K-feldspar at the solidus are greatly increased at 10 kbar compared with those at 1 atm. The maximum solubility of K-feldspar in anorthite is *c.* 5% at 1 atm, *c.* 18% at 10 kbar; and that of anorthite in K-feldspar is *c.* 3% at 1 atm, *c.* 7% at 10 kbar. The increased solubilities are attributed to the increase in the eutectic temperature at high isostatic pressures. The results imply increased ternary feldspar solid solutions at high pressures and support the existence of homogeneous feldspars with extensive ternary composition under high-P, T and anhydrous conditions.

KEYWORDS: anorthite, K-feldspar, phase relations, solid solutions.

Introduction

ANORTHITE, albite, and K-feldspar are the major components of most natural feldspars. Anorthite and albite form a complete solid-solution series (Bowen, 1913). Albite and K-felspar can also form a complete solid solution (Tuttle and Bowen, 1958). The solid solution between anorthite and K-feldspar is apparently very limited, although there has been no previous experimental work done in the pure anorthite–K-feldspar binary system. Phase relations in this system have been inferred from the studies of more complex systems. e.g. the study of Schairer and Bowen (1947) in the system anorthite–leucite–silica at 1 atm, and that of Yoder *et al.* (1957) in the ternary feldspar system at 5 kbar water pressure. The mutual solubilities between anorthite and K-feldspar are so limited at 1 atm that solid solution could not be detected by Schairer and Bowen (1947), who used the refractive index method to examine their run products. At $P(H_2O) = 5$ kbar and 845 °C, the maximum K-feldspar solid solution in anorthite is less than 5 mol.%, and the maximum anorthite solid solution in K-feldspar is less than 2 mol.% (Yoder *et al.*, 1957). These values are very uncertain due to the insensitivity of the X-ray diffraction method used.

Experiments carried out on the water-saturated ternary feldspar system demonstrate that anorthite solubility in K-feldspar is 5–7 mol.% (Hamilton, 1969), and K-feldspar solubility in anorthite is less than 10 mol.% (Norris, 1972) at 900 °C, 0.5 kbar water pressure. K-feldspar solubility in anorthitic plagioclase in the ternary feldspar system is about 4.4 mol.%, and anorthite solubility in potassic alkali-feldspar is about 3 mol.%, according to the experimental results of Seck (1971) at 900 °C, 0.5 kbar water pressure.

The survey of the K-feldspar content of natural plagioclases by Sen (1959) documents a maximum content of 3% in anorthitic plagioclase in granulite-facies rocks and 0.6% in amphibolite-facies rocks. The maximum anorthite content in natural potassic alkali-feldspar is 2.5% (Spencer, 1937). The solid-solution limit in the ternary feldspar system given by Brown and Parsons (1985) also indicates that the mutual solubilities between anorthite and K-feldspar are less than 10% near the anorthite–K-feldspar join. These results agree well with the above experimental data because the natural feldspars examined were homogeneous and were formed at low temperatures (<1000 °C) and low pressures (<6 kbar).

The effect of high pressure under dry conditions on ternary feldspar solid solutions is virtually

Mineralogical Magazine, June 1989, Vol. 53, pp. 337–345

unknown, and neither is that on the mutual solubilities between anorthite and K-feldspar. In the alkali-feldspar system, pressure is believed to have little effect on the position of the solvus (Tuttle and Bowen, 1958, Fig. 17). However, the melting temperatures of plagioclase and alkali feldspar are increased at high isostatic pressures (Lindsley, 1966, 1968) which, in turn, should increase the maximum feldspar solid solutions. In order to test this hypothesis a set of experiments has been conducted, the results of which form the main content of this paper.

Experimental methods

All experiments were carried out in a solid-media piston-cylinder apparatus of Boyd and England (1960) type. Pressure uncertainty is about ±0.5 kbar, and variation during experiments is negligible. Temperature was measured by a Pt/Pt(90%)Rh(10%) thermocouple and was controlled within ±15 °C for long runs (> 1 day) and within ±10 °C for runs lasting only a few hours.

The starting material for most runs was glass melted from a sintered oxide mix on an iridium-strip heater. The oxide mixes were prepared according to the desired proportions of anorthite to K-feldspar, and were mixed under acetone in an agate mortar for more than 20 minutes.

For most of the runs a layered sample assembly was used. Several glasses of different composition were placed in a single Pt capule, each separated by 2 or 3 Pt discs. Before each experiment the sample was kept in an oven at 120 °C overnight in order to drive off water absorbed by the sample during assembly preparation.

Since experiments were done under dry conditions, the feldspar melts have large viscosities, crystallization rates during experiments were extremely slow, even at temperatures as high as 1200 °C. As an example, the effect of run time on the run products is shown in Fig. 1 for the two runs (No. T-3151 and T-2151) with identical starting composition: Kf# = 25 [Kf# = 100 Kf/(Kf + An)]. Both runs were carried out at 1200 °C. The T-2131 run, of three hours duration, produced only small and poorly-formed anorthite crystals, manifested as the weak anorthite peaks in the X-ray diffraction pattern (Fig. 1*a*). This contrasts with the well developed anorthite peaks of run T-2151 of eleven days duration (Fig. 1*b*). More importantly, the XRD pattern for run T-2151 reveals the presence of K-feldspar crystals, which are not seen in the pattern of run T-2131 (K-feldspar peaks are shaded in Fig. 1*b*). Consequently run times were carefully chosen at each

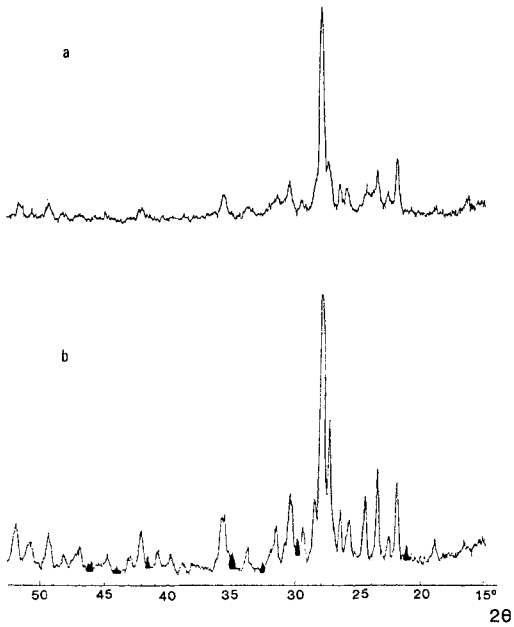

FIG. 1. The XRD patterns of two runs at 1200 °C with identical starting composition, showing time effect on the run products: (*a*) T-2131 (3 hours); (*b*) T-2151 (11 days).

temperature, based on the experience of Schairer and Bowen (1947) from experiments in the anorthite–leucite–silica system, and on experience gained in the first few experiments of this study. It was found that the required run time increased from a few hours at temperatures between 1400 and 1600 °C, to a few days at temperatures 1200–1300 °C, and to 10–20 days at temperatures less than 1200 °C.

Experimental results

Microscope examination. Run products were first examined with an optical microscope. It was very difficult to distinguish anorthite from K-feldspar (although they could sometimes be distinguished by their relief difference). The refractive index (RI) of the oil chosen was 1.550, falling between 1.53 (RI of pure K-feldspar) and 1.580 (RI of Anorthite). Observation of relative relief was hampered by the small size of crystals and probably due to solid solution, which tended to decrease the RI of anorthite and increase that of K-feldspar. The presence and amount of melt were very difficult to estimate microscopically; however, the existence of a large amount of melt could be recognized. The glass was brittle and,

when crushed, very small pieces were readily obtained. Crystal-dominated samples needed to be crushed many times into the sufficiently small pieces required for SEM observation.

XRD analysis. After microscopic observation, the crushed powder was examined by X-ray diffraction techniques. To keep the samples pure for further infra-red investigation, an internal standard was not used. The consistency of the XRD results was checked by repetitive analysis of the same sample. All diffraction patterns indicate that no other minerals except feldspars are present in the run products. All run products are, therefore, believed to contain only feldspars and/or their equivalent glasses.

A smear amount of sample was scanned between 15 and 52° (2θ) on a Philips diffractometer using Cu-$K\alpha$ radiation. Typical XRD patterns are shown in Fig. 2. The first pattern (Fig. 2*a*) shows the presence of K-feldspar only (shaded are diagnostic K-feldspar peaks). The second (Fig. 2*b*) indicates both anorthite and K-feldspar present as run products. The third (Fig. 2*c*) is identical to the pure anorthite pattern.

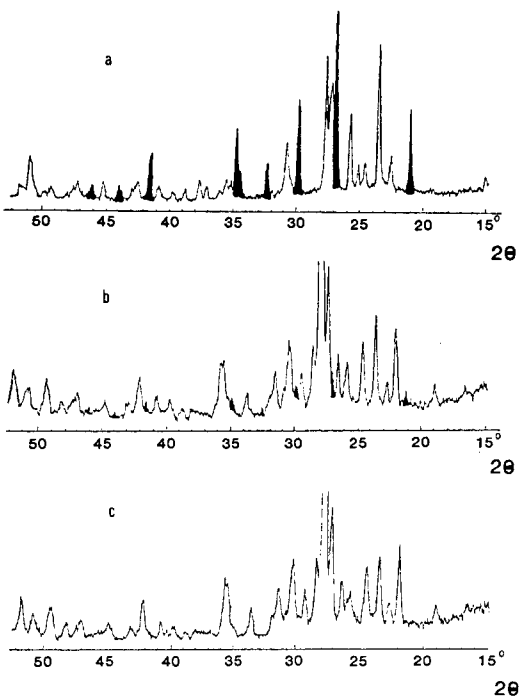

FIG. 2. Three typical XRD patterns of the run products: (*a*) T-2152 1200 °C Kf_{90} K-feldspar only; (*b*) T-2151 1200 °C Kf_{25} anorthite and K-feldspar; (*c*) T-2155 1200 °C Kf_{20} anorthite only.

Since the strongest K-feldspar peaks (2θ between 27 and 28°) are often obscured by the strongest anorthite peaks, they are not diagnostic. Fortunately other peaks do not all overlap.

Among the diagnostic peaks, the ($\bar{2}01$) K-feldspar peak (*c.* 21°) and the ($\bar{2}02$) anorthite peak (*c.* 22°) are the 'characteristic' peaks for K-feldspar and anorthite respectively. It is often necessary to check the presence of other peaks beside the two characteristic peaks before making a final conclusion as to which feldspar is present and which is not, especially when the peaks are very weak (either due to the small amount of sample available or small amount of crystals present).

Several methods have been proposed to determine synthetic feldspar composition by the XRD powder method, such as the [2θ ($\bar{2}01$) of feldspar–2θ ($10\bar{1}0$) of quartz]–K-feldspar wt.% method of Tuttle and Bowen (1958); the [4θ ($\bar{2}04$)–4θ (060)–anorthite wt.% method of Viswanathan (1971). These methods have been used by some researchers in experimental studies (e.g. Seck, 1971; Yoder *et al.*, 1957), but their accuracy has been questionable (e.g. Norris, 1972). In this study, the XRD method has been used to check for the presence of phases in the run products only. The compositions of these phases were determined by electron microprobe analysis (see below).

The absence of feldspar crystals, or the presence of one or two feldspars in a XRD chart of a run product is used to fix the liquidus and solvus positions. The limiting factor is the detection limit of this X-ray method. In order to evaluate this limit, natural feldspars of known composition (sanidine and An-rich plagioclase) were mechanically mixed in different proportions and were analysed by the X-ray diffractometry. The sanidine was separated from a course-grained porphyry from Port Cygnet, Tasmania. Its composition is $(K_{0.82}Na_{0.13}Ca_{0.04})AlSi_3O_8$ (sample CY13 of Ford, 1983). The plagioclase [$(Ca_{0.93}Na_{0.07})Al_2Si_2O_8$] was separated from a dredged basaltic lava from the north Tonga ridge (sample No. D3–52 of Falloon, unpublished data). For a mixture of the above sanidine (5%) and plagioclase (95%), the ($\bar{2}01$) peak of sanidine and other peaks were sometimes but not always obvious in the XRD charts for repetitive XRD analyses. For a mixture of 10% sanidine and 90% plagioclase the ($\bar{2}01$) and other sanidine peaks are clearly shown in the chart. Thus the detection limit of this method is approximately 5%. This limit is important when two feldspars are present in a run product, and when determination of the position of the solvus

is concerned. The results of the XRD analysis are given in Table 1.

SEM observation. A polished microprobe mount of run products was observed with a Philips 505 Scanning Electron Microscope (SEM). Phases present in the run products could not be distinguished by back-scattered or secondary electron images because of small difference in mean atomic number between these phases. To avoid this problem, a sample was etched with HF acid (1 wt.% HF solution) at room temperature for about 1 minute. Acid-etching produced marked surface relief (Fig. 3*a*) with glass being readily dissolved by the HF-solution, highlighting the remaining etch-resistant surfaces of crystals. However, in samples without glass, etching may have occurred along the boundaries between crystals, resulting in very irregular boundaries of these crystals. Any interpretation of Fig. 3*a* is thus equivocal; it may infer that the charge contains at least two phases, but whether one is glass or both are crystals is not certain as individual crystals cannot be identified. Furthermore, when the sample was analysed by electron microprobe after etching, analyses were always poor. The total oxide weight percent was less than 80%, and the cation sum per 8 oxygens as high as 7.00. The etching technique was therefore not helpful.

Another technique was adopted in order to determine the phases present in run products. This was called the 'broken surface' technique. After each experiment the run product was crushed and some small chips were picked up, coated with gold, and observed under the SEM. A back-scattered electron image revealed the detailed surface morphology of a broken chip (Fig. 3*b*). Although the sample was the original run product and was not etched, there are many holes between the obvious crystals in Fig. 3*b*. Such an image is considered to show typical subsolidus features. It is clear that all the crystals are indeed very small (about 5 μm by 2–3 μm). In hypersolidus runs the crystals (with regular shape) stand out because they are harder than glass. Sometimes regular voids were left on the surface where crystals had been plucked during crushing (Fig. 3*c*). Occasionally, a kind of 'step-like' feature within a crystal can be seen (Fig. 3*d*). The 'steps' are probably cleavages. In contrast, glass always appears smooth, sometimes showing conchoidal fracture.

For runs very close to the solidus, traces of melt are very difficult to recognize from SEM images. In such cases, identification of glass was made by electron microprobe analysis of the run products.

Electron microprobe analysis (EMPA). Run products and their starting material (glass) were

Table 1 Experimental Results

Run No.	Start Com I	Start Com A	T °C	Run Duration	Run Product XRD	Run Product SEM	Run Product EMPA Range
T-2080	25	24.0	1600	0.5h	no peak	M	23.7 - 24.4
T-2130	25	24.2	1550	1.5h	no peak	M	23.7 - 24.7
T-2127	50		1500	2h	no peak	M	
T-2127	40		1500	2h	no peak	M	
T-2062	30	29.5	1500	2h	An peaks	M & C	26.7 - 33.4
T-2057	20	19.7	1500	1h	An peaks	M & C	12.4 - 23.8
T-2057	10	10.0	1500	1h	An peaks	M & C	4.9 - 15.2
T-2060	10	10.5	1500	3h	An peaks	M & C	5.6 - 15.0
T-2070	5	4.8	1500	2h	An peaks	C & M	2.9 - 7.5
T-2125	60		1400	3.6h	no peak	M	
T-2061	50	48.9	1400	3h	An peaks	M & C	45.3 - 50.8
T-1996	40	38.4	1400	5.2h	An peaks	M & C	26.9 - 47.6
T-1996	30	27.2	1400	5.2h	An peaks	M & C	16.2 - 39.9
T-2017	30	28.2	1400	5h	An peaks	M & C	25.2 - 34.0
T-1996	20	20.5	1400	5.2h	An peaks	C & M	14.1 - 22.8
T-2073	15	14.4	1400	3h	An peaks	C & M	11.3 - 15.6
T-1996	10	10.0	1400	5.2h	An peaks	C (+ M?)	7.0 - 11.7
T-2134	60		1300	6.6h	An peaks	M (+ C?)	
T-1984$	50	48.8	1300	2d		M (+ C?)	42.0 - 60.8
T-1984$	40	38.3	1300	2d		M & C	27.3 - 61.2
T-1984$	30	29.0	1300	2d		C & M	19.0 - 42.8
T-2090$	30	29.2	1300	8d	An peaks	C & M	25.1 - 39.6
T-2071	25	25.2	1300	8h	An peaks	C & M	18.3 - 31.2
T-1984$	20	19.9	1300	2d	An peaks	C (+ M?)	16.9 - 23.4
T-1736	9.5	9.4	1300	2d	An peaks	C	5.6 - 12.9
T-1736	5.6	5.6	1300	2d	An peaks	C	1.5 - 7.9
T-2148	80	78.0	1250	2d	Kf peaks	M & C	72.5 - 85.9
T-2172	50	47.6	1250	10d	An peaks	M & C	18.2 - 35.5
T-2172	25	23.9	1250	10d	An peaks	C & M	16.5 - 28.6
T-2122	25	23.8	1250	2d	An peaks	C & M	20.2 - 26.4
T-2160	70		1225	6d 1h	An & Kf peaks	C & M	
T-2135	30	29.9	1225	3d 22.5h	An peaks	C & M	18.9 - 30.4
T-2152	90	89.7	1200	7d	Kf peaks	C	88.3 - 94.0
T-2152	80	77.4	1200	7d	Kf & An peaks	C (+ M?)	69.6 - 92.8
T-1933$	60	54.4	1200	10d 18h		M & C	16.8 - 69.8
T-1933$	50	48.5	1200	10d 18h		M & C	16.3 - 68.0
T-1933$	40	38.4	1200	10d 18h		M & C	16.4 - 65.2
T-1933$	30	30.6	1200	10d 18h	An(+ Kf?) peaks	C & M	17.0 - 60.5
T-2131	25		1200	3h	An(+ Kf?) peaks	C & M	16.3 - 53.2
T-2151	25		1200	11d 12h	An & Kf peaks	C (+ M?)	
T-2155	25		1200	11d 18h	An & Kf peaks	C (+ M?)	16.9 - 35.9
T-2155	20	20.5	1200	11d 18h	An peaks	C (+ M?)	16.4 - 22.9
T-1887$	20	19.5	1200	10d	An peaks	C (+ M?)	16.4 - 24.4
T-1887$	9.5	9.2	1200	10d		C	5.4 - 8.1
T-1765$	9.5	8.3	1200	6d 22h		C	4.6 - 11.2
T-1740	9.5	9.5	1200	7d		C	4.2 - 12.8
T-1887$	5.6	5.9	1200	10d		C	3.6 - 6.2
T-2105	50	49.1	1175	13d	Kf & An peaks	C	27.6 - 70.7
T-1987$	60	56.8	1150	7d	An & Kf peaks	C	38.2 - 71.9
T-1987$	50	49.1	1150	7d	An & Kf peaks	C	31.4 - 71.4
T-1987$	40	39.3	1150	7d	An & Kf peaks	C	17.6 - 65.5
T-1987$	30	30.3	1150	7d	An & Kf peaks	C	21.9 - 77.2
T-2142$	25	24.1	1150	7d 22.5h	An & Kf peaks	C	18.3 - 34.4
T-2149	25	24.5	1150	3d	An & Kf peaks	C	18.3 - 41.5
T-2156	25	24.8	1150	8d	An + Kf peaks	C	22.7 - 43.4
T-2118	20	20.2	1150	2d 3h	An peaks	C	16.1 - 30.1
T-2153	25	24.5	1100	1d 12h	An & Kf peaks	C	17.1 - 49.3
T-2147	20	20.4	1100	14d 16h	An & Kf peaks	C	15.2 - 39.5
T-1830$	9.5	10.1	1100	13d	An peaks	C	5.3 - 14.2
T-1830$	5.6	6.1	1100	13d	An peaks	C	1.9 - 10.5
T-2158	20		1050	20d	An & Kf peaks	C	
T-2066	50		1000	4h	An & Kf peaks	C	
T-2154	20		950	11d	An & Kf peaks	C	
T-2154	15		950	11d	An & Kf peaks	C	
*	*	*	*	*	Reversal Runs	*	*	*	*
T-2264 (T-2155)	20		1050	15d	An & Kf peaks		
T-2285 (crystalline)	20		1200	20d	An peaks		

1) '$' indicates salt/pyrex assembly; the rest, talc/pyrex assembly
2) All compositions are given as Kf# [= 100*Kf/(Kf + An)].
'Start Com': starting composition; 'I': initial composition;
'A': actual composition given by electron microprobe analysis.
3) Under 'Run Duration' d: day; h: hour.
4) Under 'SEM' M: melt; C: crystals.

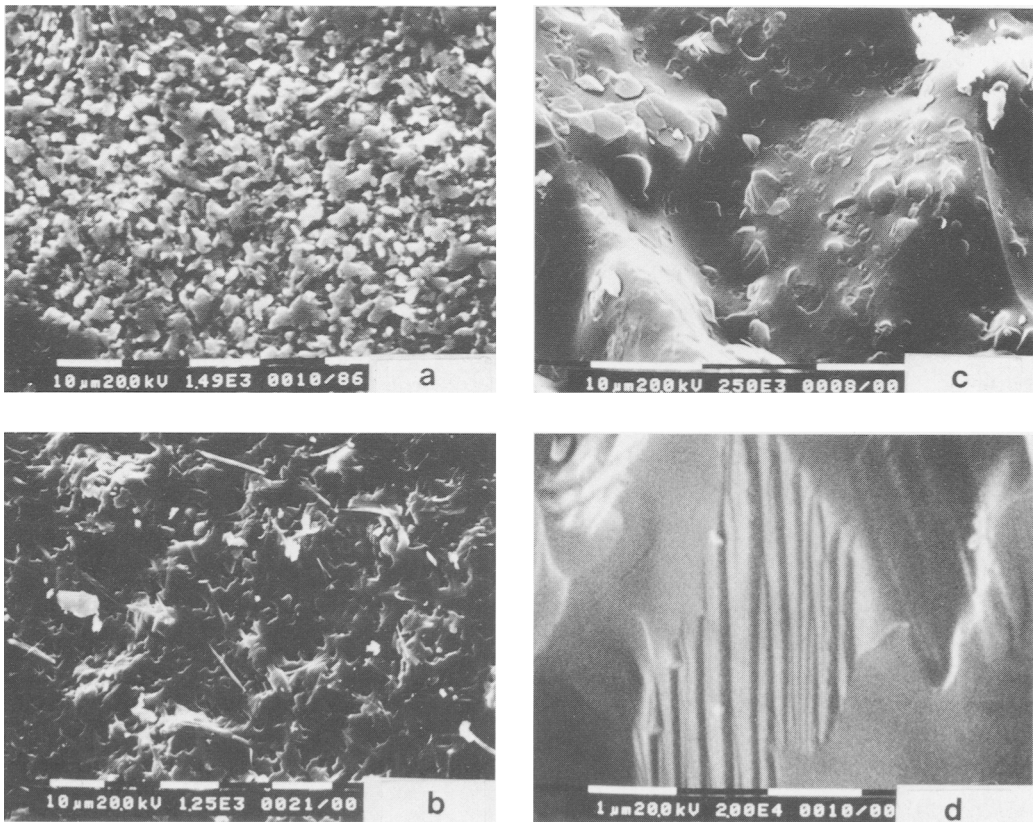

FIG. 3 (*a* and *b*). Back-scattered electron (BSE) images of run product of run T-1987 (1150 °C, Kf_{60}): (*a*) HF-etched; (*b*) broken surface. (*c*) BSE image of run product of run T-1933 (1200 °C, Kf_{40}) showing coexisting crystals and melt on a broken surface (note voids suggesting prior crystal positions). (*d*) BSE image of run product of run T-1933 (1200 °C, Kf_{60}) displaying cleavages in a synthetic feldspar crystal.

analysed by a JEOL JX–50A electron probe microanalyser with an EDX system. Normal beam current was 7.0×10^{-10} A on a Cu metal standard, with an accelerating voltage of 15 kV.

Both focussed-beam (spot) analysis of the glass starting material and defocussed-beam (area scan) analysis of the products show consistent Kf#, which varies within the limit of ±3 (Kf#). The actual bulk composition of each run product seems to have slightly less Kf# than the initial bulk composition of its oxide mix (compare columns 'A' and 'I' in Table 1). K loss probably occurred during glass preparation, rather than during the microprobe analysis process, because the glass analyses show consistent Kf#.

The compositional range of the individual run product is given in Table 1 under 'EMPA Range'. Although it was not possible to avoid overlap between phases, these compositional ranges are used to define the phase boundaries (i.e. the liquidus, solidus, and solvus). In any composition midway between phase boundaries at a particular temperature, it is clear that all analyses are mixtures of very small crystals, or crystals and melt. If the bulk compositions of the run products are very close to a phase boundary, their extreme (minimum or maximum) Kf# should lie near the phase boundary. For example, at 1300 °C the maximum Kf# in the analyses of run products with bulk compositions 50 and 40 (Kf#, initial composition) is *c.* 61, which is taken as the liquids composition at 1300 °C. Such a treatment is justified by the consistency among the analytical data and by the observations obtained by other methods mentioned above.

Clearly no one given method of analysis of these experiments is adequate to unequivocally define the phase boundaries. Based on the XRD analy-

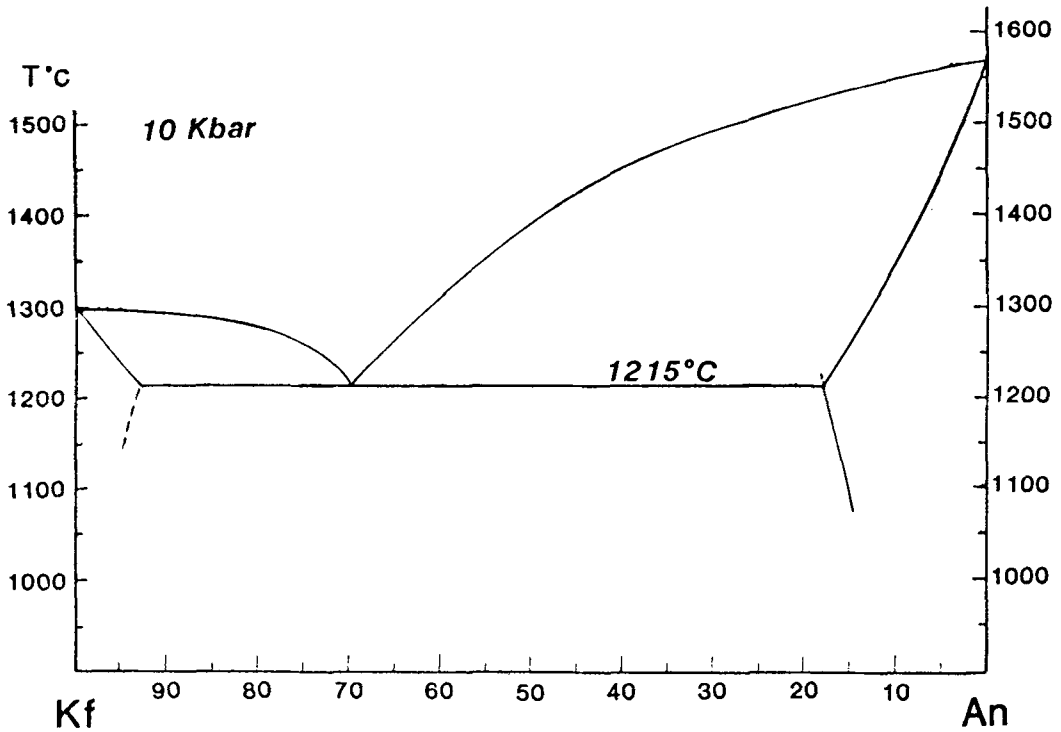

FIG. 4. Phase relations in the binary system anorthite–K-feldspar at 10 kbar. The eutectic point is at 1215° ± 15 °C, 70 ± 3(Kf#). Solid solutions: Kf in An 18 ± 3%; An in Kf 7 ± 3%.

sis, SEM observation, and the EMPA results, the phase diagram in the binary system anorthite–K-feldspar was constructed in Fig. 4. The phase relations between anorthite and K-feldspar are of eutectic type with the eutectic point located at 1215° ± 15 °C, and Kf# 70 ± 3. The maximum solubility of K-feldspar in anorthite is 18 ± 3% and that of anorthite in K-feldspar is 7 ± 3%. The melting temperatures of pure anorthite and K-feldspar at 10 kbar are 1575 °C (Goldsmith, 1980) and 1300 °C (Lindsley, 1966) respectively.

Evaluation of attainment of equilibrium

In melting experiments in the systems Ab–An–H_2O and the Qz–Ab–An–H_2O at 5 kbar water pressure, Johannes (1978) observed that reaction rates are extremely sensitive to temperature; a change in temperature of 100 °C resulting in a change in the reaction rate of several orders of magnitude. At 1000 °C in the Ab–An–H_2O system, equilibrium is believed to be reached in 1 hour, while at 800 °C the reaction was considered to be too slow to reach equilibrium within reasonable experimental time. In the system Qz–Ab–An–H_2O, plagioclase approached equilibrium compositions very slowly, and extrapolation to 730 °C shows that 100 000 years are needed to achieve equilibrium.

In an experimental study of the ternary feldspar system, Johannes (1979) used synthetic feldspar as the starting material and found that equilibrium was reached after 10 days at 800 °C and 20 days at 650 °C, at 1 kbar water pressure. This was orders of magnitude faster than the reactions that had occurred in his previous melting experiments.

The reactions in the melting experiments (Johannes, 1978) were hypersolidus, and those in the ternary feldspar experiments (Johannes, 1979), subsolidus. It is generally believed that hypersolidus reactions should be faster than subsolidus reactions because melt is involved in the hypersolidus reactions and ions move faster in melt than in solid. However, the reaction rates noted above, in the melting and the ternary feldspar experiments, are opposite to those predicted. This problem was acknowledged by Johannes (1979), although he could offer no simple explanation. It was also observed that the rate of a reac-

tion leading to a more An-rich plagioclase is much faster than a reaction producing a more Ab-rich plagioclase. This was suggested to be due to the 'obstacle effect' of albite, which blocks the spaces for transportation of reactants (Johannes, 1979). If this is true, then reactions in the binary system anorthite–K-feldspar should reach equilibrium easier than those in systems involving albite.

In the present experiments reaction rates may have been accelerated by enhanced H_2 activity, resulting from the use of talc/pyrex assemblies. The presence of H_2 during experiments, generated through OH breakdown from talc at high-P, T, has the effect of promoting Al–Si interdiffusion (Goldsmith, 1986), and thus can help to achieve more rapid equilibrium in the anorthite–K-feldspar reaction.

Reversal experiments were undertaken to confirm the phase relations shown in Fig. 4. These experiments were focussed on the maximum K-feldspar solubility in anorthite, which occurs at the eutectic temperature. Two types of reversal experiments were performed in order to bracket the solvus; one was an exsolution experiment using anorthite with the maximum K-feldspar solid solution, and the other was a synthesis experiment of such anorthite from pure crystalline anorthite and K-feldspar starting material. For the first experiment (T-2264), the temperature chosen was 1050 °C so as to reach equilibrium during the short run time (15 days) and to produce sufficient K-feldspar to be detected by the XRD method. The starting material was the run product of T-2155, believed to contain only anorthite with the maximum K-feldspar solid solution (20%) at 10 kbar. Figure 4(*a*) shows part of the XRD pattern of the starting material, in which the diagnostic ($\bar{2}01$) peak of K-feldspar is not present, nor any other K-feldspar peaks. In the reversal run an obvious peak at 20.8° (2θ) occurs in the XRD pattern (Fig. 5*b*), clearly indicating the presence of exsolved K-feldspar together with anorthite in the run product. This means that the high temperature anorthite (with 20% K-feldspar solid solution) decomposed into two phases at lower temperature.

In the second reversal experiment a mixture of synthetic anorthite (80%) and K-feldspar (20%) was used as the starting material. Anorthite was synthesized at 1050 °C and 10 kbar for 10 hours in a Ag_{50} Pd_{50} capsule from an oxide mix of CaO, Al_2O_3, and SiO_2. About 7 wt.% water was added to the oxide mix in order to promote crystallization. K-feldspar was synthesized at 1100 °C and 25 kbar over 22 hours from an oxide mix of K_2O, Al_2O_3, and SiO_2 in a graphite capsule (K_2O was the decomposition product of K_2CO_3).

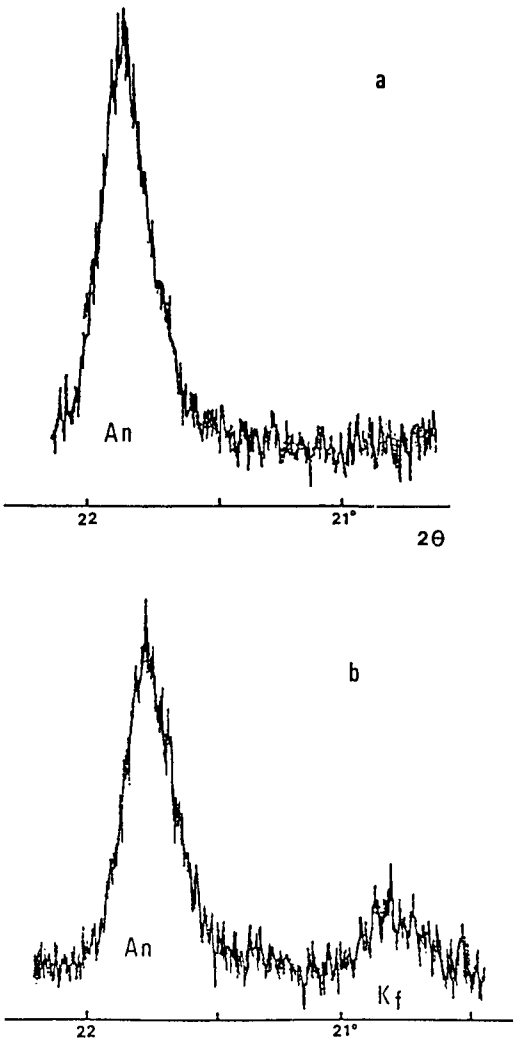

FIG. 5. Part of the XRD patterns of (*a*) the starting material (product of the run T-2155); and (*b*) the run product of the reversal run T-2265 at 1050 °C.

No flux was added. The purity of the synthetic anorthite and K-feldspar was checked by the XRD method. No other phases except anorthite and K-feldspar were found. The synthetic anorthite (80%) and K-feldspar (20%) were mechanically mixed in an agate mortar for more than 20 minutes. The mix was placed in an oven at 120 °C overnight and then run at 1200 °C and 10 kbar for 20 days in a Pt capsule (run T-2285). The XRD patterns of the starting material and the run product are shown in Fig. 6, clearly illustrating the presence of both anorthite and K-feldspar in the

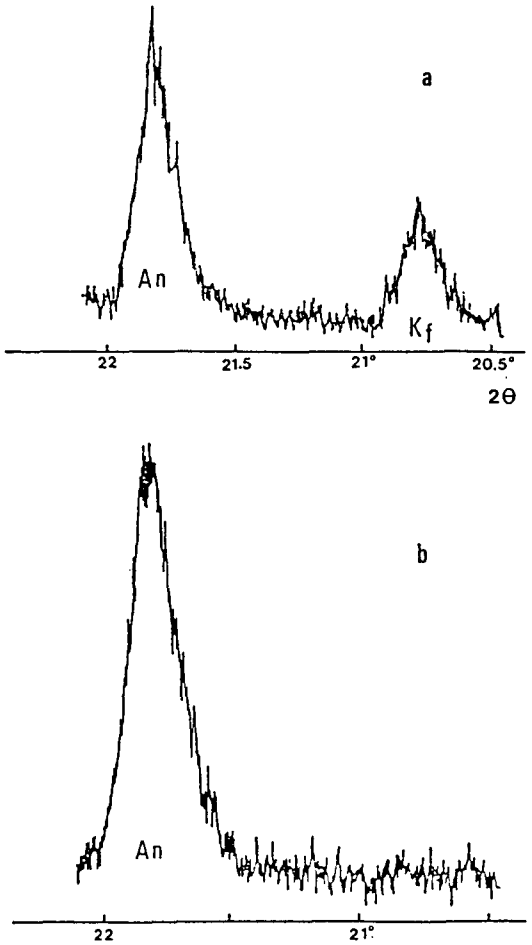

FIG. 6. Part of the XRD patterns of (*a*) a mechanical mix of 80% anorthithe + 20% K-feldspar (the starting material) and (*b*) the run product of T-2285 at 1200 °C.

former, while only anorthite (with 20% Kf) is present in the latter. The 20% K-feldspar has been dissolved by the anorthite. These two reversal experiments convincingly demonstrate that only one phase is present at 1200 °C and 10 kbar for the composition Kf_{20} An_{80}, and prove the attainment of equilibrium during experiments.

Conclusions and possible application

This study shows that the mutual solubilities between anorthite and K-feldspar are much increased at high isostatic pressure: from 5% at 1 atm to 18% at 10 kbar for K-feldspar in anorthite, and from 3% at 1 atm to 7% at 10 kbar for anorthite in K-feldspar. The increase in the mutual solubilities is probably due to the increased eutectic temperature caused by the increased pressure. Pressure itself may have no effect on the mutual solubility because no change in the solvus is observed at a given temperature and at different pressures. This is consistent with the observations of Tuttle and Bowen (1958) in the alkali feldspar system.

The increased solid solutions in the binary system anorthite–K-feldspar imply that the ternary feldspar solid solutions must be increased at high isostatic pressures. This may give an alternative explanation for the origin of some ternary feldspar intergrowths. Although having strong ternary compositions, some ternary feldspar intergrowths may be a result of exsolution. Homogeneous feldspar with extensive ternary compositions may exist at high pressures and high temperatures. As an example, some ternary feldspar intergrowths in two basaltic dykes found in Departure Rocks, Antarctica, show strong petrographic and geochemical evidence for their origin by exsolution (Ai *et al.*, in preparation). These intergrowths have an averaged bulk composition $Kf_{21.5}$ An_{64} $Ab_{14.5}$, which is believed to be the composition of the homogeneous parental feldspar. The existence of such a parental feldspar at elevated pressure is supported by the experimental results reported in this study. Experiments in the ternary feldspar system are necessary to prove this suggestion. These results will be discussed in another paper.

Acknowledgements

We thank Dr W. R. Taylor for valuable suggestions and discussions; Dr E. Takahachii for suggesting the use of HF-etching technique; Messrs K. L. Harris and W. Jablonski for technical assistance. Mr. J. D. Adam, Mr S. M. Eggins and Dr A. J. Crawford are thanked for proof-reading the manuscript. Financial support came from the State Education Commission of the People's Republic of China (YA) and ARCS research grant (DHG).

References

Bowen, N. L. (1913) *Am. J. Sci.* **35,** 577–99.
Boyd, F. R., and England, J. L. (1965) *J. Geophys. Research,* **65,** 741–8.
Brown, W. L., and Parsons, I. (1985) *Am. Mineral.* **70,** 356–61.
Ford, R. J. (1983) *The alkali rocks of Port Cygnet, Tasmania.* PhD thesis, University of Tasmania.
Goldsmith, J. R. (1980) *Am. Mineral.* **65,** 272–84.
——(1986) *Earth Planet. Sci. Lett.* **80,** 135–8.
Hamilton, D. L. (1969) *Progress in Experimental Petrology.* NERC publication First Report, 51–2.
Johannes, W. (1978) *Contrib. Mineral. Petrol.* **66,** 295–303.
——(1979) Ibid. **68,** 221–30.

Lindsley, D. H. (1966) *Am. Mineral.* **51,** 1793–9.
——(1968) *New York State Museum and Sci. Service Memoir,* **18,** 39–46.
Norris, G. H. (1972) *Progress in Experimental Petrology.* NERC publication, series D, No. 2, 15–19.
Schairer, J. F., and Bowen, N. L. (1947) *Geol. Soc. Finland Bull.* **20,** 67–87.
Seck, H. A. (1971) *Neues Jahrb. Mineral. Abh.* **115,** 315–45.
Sen, S. K. (1959) *J. Geol.* **67,** 479–95.
Spencer, E. (1937) *Mineral. Mag.* **24,** 453–94.
Tuttle, O. F., and Bowen, N. L. (1958) *Geol. Soc. Am. Memoir* **74.**
Viswanathan, K. (1971) *Contrib. Mineral. Petrol.* **30,** 332–5.
Yoder, S. H., Jr., Steward, D. B., and Smith, J. R. (1957) *Carnegie Inst. Washington Yearb.* **56,** 206–14.

[*Manuscript received 26 July 1988; revised 30 August 1988*]